HHS Public Access

Author manuscript

Ann Neurol. Author manuscript; available in PMC 2022 October 10.

Published in final edited form as:

Ann Neurol. 2021 November ; 90(5): 845–850. doi:10.1002/ana.26211.

Ablating the Transporter Sodium-Dependent Dicarboxylate Transporter 3 Prevents Leukodystrophy in Canavan Disease Mice

Yan Wang, PhD[1,†], **Vanessa Hull, MS**[1,†], **Sarah Sternbach, BS**[2,†], **Brad Popovich, BA**[3], **Travis Burns, BS**[1], **Jennifer McDonough, PhD**[2], **Fuzheng Guo, PhD**[1], **David Pleasure, MD**[1]

[1]Institute for Pediatric Regenerative Medicine, UC Davis, c/o Shriners Hospital, Sacramento, CA;

[2]Department of Biological Sciences and School of Biomedical Sciences, Kent State University, Kent, OH;

[3]Department of Chemistry and Biochemistry, Kent State University, Kent, OH

Abstract

Canavan disease is caused by *ASPA* mutations that diminish brain aspartoacylase activity, and it is characterized by excessive brain storage of the aspartoacylase substrate, *N*-acetyl-L-aspartate (NAA), and by astroglial and intramyelinic vacuolation. Astroglia and the arachnoid mater express sodium-dependent dicarboxylate transporter (NaDC3), encoded by *SLC13A3*, a sodium-coupled transporter for NAA and other dicarboxylates. Constitutive *Slc13a3* deletion in aspartoacylase-deficient Canavan disease mice prevents brain NAA overaccumulation, ataxia, and brain vacuolation.

Canavan disease is a vacuolar leukodystrophy caused by *ASPA* mutations that diminish brain expression of aspartoacylase, an oligodendrocyte-enriched enzyme that cleaves the abundant brain amino acid *N*-acetyl-L-aspartate (NAA) to acetate and L-aspartate. The disease usually presents in infancy, with ataxia, hypotonia, and failure to acquire developmental milestones, often in association with macrocephaly, blindness, nystagmus, and seizures. Occasionally, the clinical onset is delayed until later in childhood.[1] Magnetic resonance imaging shows alterations in brain signals indicative of cytotoxic edema and diffusion restriction[2]; proton magnetic resonance spectroscopy demonstrates a marked elevation in brain NAA concentration ($[NAA_B]$)[3]; and neuropathological studies reveal "spongiform" vacuoles arising within myelin and astroglia.[4] No therapies presently available prevent or reverse Canavan disease.

Address correspondence to Dr David Pleasure, UC Davis Department of Neurology, c/o Shriners Hospital, 2425 Stockton Boulevard, Sacramento, CA 95817. depleasure@ucdavis.edu.

†Co-first authors.

Author Contributions

Y.W., V.H., S.S., J.M., and D.P. contributed to conception and design of the study. Y.W., V.H., S.S., B.P., T.B., J.M., F.Z., and D.P. contributed to acquisition and analysis of data. Y.W., V.H., S.S., T.B., J.M., F.Z., and D.P. contributed to drafting the text or preparing the figures.

Potential Conflicts of Interest

Nothing to report.

[NAA_B] is also elevated in mice homozygous for a nonsense *Aspa* mutation. These aspartoacylase-deficient "CD mice" develop central nervous system astroglial and intramyelinic vacuolation by postnatal day (P) 14, and ataxia by P21.[5] Suppressing [NAA_B] elevation by knocking out or knocking down *Nat8l*, which encodes the neuronal NAA synthesizing enzyme *N*-acetyltransferase 8-like (*N*-acetylaspartate synthase), prevents ataxia and brain vacuolation in these mice,[6–8] supporting the hypothesis that leukodystrophy in aspartoacylase-deficient brains is a consequence of brain NAA overload.

The Na^+/dicarboxylate cotransporter sodium-dependent dicarboxylate transporter (NaDC3), encoded by *Slc13a3*, a member of the *Slc13* Na^+-coupled di- and tri-carboxylate/sulfate transporter gene family, provides the only established means to date by which mammalian cells can import NAA.[9–11] The present study surveys murine brain *Slc13a3* mRNA and immunoreactive NaDC3 expression, and evaluates the phenotypic consequences of constitutive *Slc13a3* deletion (*Slc13a3*$^{KO/KO}$) in aspartoacylase-expressing (*Aspa*$^{WT/WT}$) and CD (*Aspa*$^{Nur7/Nur7}$) mice.

Methods

Mice heterozygous for the *Aspa*^{nur7} nonsense mutation were obtained from the Jackson Laboratory (JAX:008607; Bar Harbor, ME). Heterozygous constitutive *Slc13a3*^{KO} mice were obtained from the MMRRC (MMRRC: 049666-UCD; UC Davis, Davis, CA). These 2 strains were crossed to obtain *Aspa*$^{nur7/nur7}$/*Slc13a3*$^{KO/KO}$ and *Aspa*$^{nur7/nur7}$/*Slc13a*$^{WT/KO}$ mice, referred to hereafter as CD/*Slc13a3*$^{KO/KO}$ and CD/*Slc13a3*$^{WT/KO}$ mice, respectively. *Aspa*$^{WT/WT}$/*Slc13a3*$^{WT/WT}$ and CD/*Slc13a3*$^{WT/WT}$ mice were from the same mouse colony. *Prox1*-tdTomato transgenic *Prox1* reporter (*Prox1-TdTomato*) mice were from the Jackson Laboratory (JAX:018128).[12] Mice were maintained on a C57BL/6 background in an American Association for Accreditation of Laboratory Animal Care (AAALAC)-certified vivarium, and mouse protocols were conducted in accordance with the United States Public Health Service (USPHS) Policy on Humane Care and Use of Laboratory Animals.

Accelerating rotarod testing (starting speed 4 rpm, increasing by 1.2 rpm every 10 seconds) was performed by blinded observers. Urine was collected from the mice on P60 and was treated with 0.1M KH_2PO_4 and 0.1M KCl, pH 3.75, and filtered. The eluate underwent liquid–liquid phase separation with acetonitrile, cyclohexanone, diethyl ether, and chloroform. The aqueous layer was collected for high-performance liquid chromatography analysis as previously described.[8]

For biochemical and histological studies, mice were deeply anesthetized with ketamine/xylazine and perfused with cold phosphate-buffered saline (PBS). Forebrain, cerebellar, spinal cord, and kidney sections were flash-frozen in liquid nitrogen for mRNA, protein, and NAA assays.[8] For immunohistology, samples of forebrain and cerebellum were postfixed in 4% paraformaldehyde in PBS, cryoprotected in 30% sucrose, embedded in optimal cutting temperature (OCT) compound, and frozen. Cryostat sections were immunostained for NaDC3 (RRID AB_2868533), vimentin (RRID AB_10003206), myelin basic protein (MBP) (RRID AB_10655672), glial fibrillary acidic protein (GFAP) (gift from V. Lee, University of Pennsylvania), or collagen 1α1 (RRID AB_10891543), counterstained with

4',6-diamidino-2-phenylindole (DAPI), and imaged on a Nikon A1 laser scanning confocal microscope. Cerebellar and thalamic white matter vacuole areas were measured using the NIS-Elements Annotate and Measure tool (Nikon).[8]

Mixed glial cell preparations were prepared from forebrains of P0 to P2 mouse pups, used to prepare astroglia-enriched cultures (92 ± 2% $GFAP^+$; n = 3, mean ± SEM) by differential shaking. Samples of kidney cerebellum, microdissected forebrain meninges and choroid plexus,[13] and harvested astroglia-enriched cultures, were assayed for mRNAs by quantitative RT/PCR. Primer pairs were as previously described,[14] with the exception that primer pairs for *Slc13a3* were forward, 5′-CTAGGAGGTGGCTTTGCC-3′; and reverse, 5′-ACTCCGTGAAGAAGGCGATG-3′. Quantitative RT/PCR results were normalized to *Hsp90* mRNA abundance. Cerebellar NAA content was assayed by high-performance liquid chromatography and expressed in micromoles per gram tissue wet weight.[8] Quantitative data are presented in the figures as means ± SEM, and statistical analyses were by 1- and 2-way ANOVA with the Tukey post-hoc test.

Results

Figure 1 quantifies and localizes brain *Slc13a3*/NaDC3 expression in $Aspa^{WT/WT}$ mice. We confirmed a prior report that cultured astroglia express *Slc13a3* mRNA[11] and, in cryostat sections of adult murine forebrain, detected faint NaDC3 immunoreactivity in $GFAP^+$ astroglia, but not in other parenchymal cells. *Slc13a3* mRNA abundance in adult mouse forebrain meninges was 20-fold higher than in mouse astroglial cultures. Immunoreactive NaDC3 in the meninges was confined to the arachnoid mater and, in *Prox1-TdTomato Prox1* reporter mice, was expressed by arachnoid cells that were co-labelled with TdTomato.

Figure 2 demonstrates a lack of effect of homozygous constitutive *Slc13a3* disruption ($Slc13a3^{KO/KO}$) on cerebellar myelination in $Aspa^{WT/WT}$ mice. Between P7 and P60, cerebellar levels of immunoreactive PDGFRα, Sox10, TCF7L2, MAG, and MBP proteins in $Aspa^{WT/WT}/Slc13a3^{KO/KO}$ mice did not differ significantly from those in $Aspa^{WT/WT}/Slc13a3^{WT/WT}$ mice, and patterns of P60 cerebellar MBP immunostaining in $Aspa^{WT/WT}/Slc13a3^{KO/KO}$ and $Aspa^{WT/WT}/Slc13a3^{WT/WT}$ mice were indistinguishable. Also between P7 and P60, there were no significant differences between $Aspa^{WT/WT}/Slc13a3^{KO/KO}$ and $Aspa^{WT/WT}/Slc13a3^{WT/WT}$ mice in spinal cord abundances of *Nat8l*, *Gfap*, *Pdgfrα*, *Tcf7l2*, *Mag*, and *Mbp* mRNAs. In fact, the only phenotypic effect of constitutive $Slc13a3^{KO/KO}$ we detected in $Aspa^{WT/WT}$ mice was a substantial elevation in urinary NAA concentration (Fig 3A).

Figure 3 illustrates the effects of $Slc13a3^{KO/KO}$ in CD mice. Urinary NAA concentrations, already elevated in the $CD/Slc13a3^{WT/WT}$ mice, were substantially increased further in $CD/Slc13a3^{KO/KO}$ mice (see Fig 3A). Notably, $Slc13a3^{KO/KO}$, although not altering *Nat8l* mRNA abundance in the CD mice, normalized [NAA_B], increased their weight at P60 and their accelerating rotarod retention times, and prevented cerebellar and thalamic vacuolation. Heterozygous *Slc13a3* deletion in CD mice also suppressed [NAA_B] elevation, enhanced accelerating rotarod performance, and partly prevented cerebellar but not thalamic vacuolation. Abundances of cerebellar oligodendroglial lineage mRNAs did

not differ significantly between *Aspa*$^{WT/WT}$/*Slc13a3*$^{WT/WT}$, *Aspa*$^{WT/WT}$/*Slc13a3*$^{KO/KO}$, CD/*Slc13a3*$^{WT/WT}$, and CD/*Slc13a3*$^{KO/KO}$ mice.

Discussion

Almost all NAA in normal brains is stored within neurons.[15] Where the additional NAA in Canavan disease and CD mouse brains accumulates has not yet been established, but the prominent astroglial vacuolation in aspartoacylase-deficient brains suggests that at least some of this additional NAA becomes sequestered within and, in conjunction with cotransported Na^+, perturbs osmolar homeostasis of NaDC3-expressing astroglia. If so, then [NAA_B] normalization and prevention of vacuolation in CD mice by constitutive *Slc13a3*$^{KO/KO}$ might represent the combined effects of accelerated brain export of non-neuronal NAA that was prevented from entering astroglia by astroglial NaDC3 ablation and enhanced renal NAA excretion owing to deletion of renal proximal tubular NaDC3.

Meningeal lymphatic vessels are a major route of cerebrospinal fluid drainage from the brain,[16] and lymphatic endothelial cells can be identified by their expression of the transcription factor Prox1.[17] By analogy with the kidney, in which tubular epithelial cell NaDC3 limits urinary excretion of NAA, α-ketoglutarate, and other dicarboxylates,[9,18] resorption of NAA from the cerebrospinal fluid by $Prox1^+$/$NaDC3^+$ arachnoid cells might contribute to [NAA_B] elevation in CD mice. *Slc13a3* conditional deletion studies would permit evaluation of the respective contributions of astroglial and arachnoidal NaDC3 ablation in suppressing this [NAA_B] elevation.

Gene therapies to prevent leukodystrophy in CD mice by driving brain expression of functional aspartoacylase are already available,[19,20] but have not yet been scaled up successfully to human brains.[3] Development of a druggable *Slc13a3* or NaDC3 inhibitor might provide a more readily translatable therapeutic approach than gene therapy for infants and children with Canavan disease. Such an inhibitor would probably not affect developmental brain myelination adversely, because myelination in *Slc13a3*$^{KO/KO}$ mice did not differ significantly in time course from that in *Slc13a3*$^{WT/WT}$ mice. A prior study demonstrating that lowering [NAA_B] in young adult CD mice by intracisternal administration of an *Nat8l* antisense oligonucleotide temporarily reversed established brain vacuolation and motor deficits[8] suggests that such an *Slc13a3* or NaDC3 inhibitor could be beneficial in children with Canavan disease who are already symptomatic. A cautionary note, however, is that although *Slc13a3*$^{KO/KO}$ was well tolerated in *Aspa*$^{+/+}$ and CD mice, a recent publication described 2 unrelated children with *SLC13A3* mutations limiting NaDC3 activity who presented with acute reversible episodes of leukoencephalopathy triggered by infections.[18]

Acknowledgments

This study was supported by NIH 1R21117386 (DP) and UL1 TR001860 (VH); Shriners grants 84553-NCA-18 (YW), 87400-NCA-21 (YW), and 85113-NCA-18 (DP); and the Dana Foundation (DP).

References

1. Bley A, Denecke J, Kohlschutter A, et al. The natural history of Canavan disease: 23 new cases and comparison with patients from the literature. Orphanet J Rare Dis 2021;16:227. [PubMed: 34011350]
2. Merrill ST, Nelson GR, Longo N, Nonkowsky JL. Cytotoxic edema and diffusion restriction as an early pathoradiologic marker in Canavan disease: case report and review of the literature. Orphanet J Rare Dis 2016;11:169. [PubMed: 27927234]
3. Leone P, Shera D, McPhee SW, et al. Long-term follow-up after gene therapy for canavan disease. Sci Transl Med 2012;4:165ra163.
4. Adachi M, Schneck L, Cara J, Volk BW. Spongy degeneration of the central nervous system (Van Bogaert and Bertrand type; Canavan's disease). A review. Hum Pathol 1973;4:331–347. [PubMed: 4593851]
5. Traka M, Wollmann RL, Cerda SR, et al. Nur7 is a nonsense mutation in the mouse aspartoacylase gene that causes spongy degeneration of the CNS. J Neurosci 2008;28:11537–11549. [PubMed: 18987190]
6. Guo F, Bannerman P, Mills Ko E, et al. Ablating N-acetylaspartate prevents leukodystrophy in a Canavan disease model. Ann Neurol 2015;77:884–888. [PubMed: 25712859]
7. Maier H, Wang-Eckhardt L, Hartmann D, et al. N-acetylaspartate synthase deficiency corrects the myelin phenotype in a Canavan disease mouse model but does not affect survival time. J Neurosci 2015;35:14501–14516. [PubMed: 26511242]
8. Hull V, Wang Y, Burns T, et al. Antisense oligonucleotide reverses leukodystrophy in Canavan disease mice. Ann Neurol 2020;87: 480–485. [PubMed: 31925837]
9. Bergeron MJ, Clemencon B, Hediger MA, Markovich D. SLC13 family of Na+-coupled di- and tri-carboxylate/sulfate transporters. Mol Aspects Medicine 2013;34:299–312.
10. Huang W, Wang H, Kekuda R, et al. Transport of N-acetylaspartate by the Na^+-dependent high-affinity dicarboxylate transporter NaDC3 and its relevance to the expression of the transporter in the brain. J Pharmacol Exp Ther 2000;295:392–403. [PubMed: 10992006]
11. Fujita T, Katsukawa H, Yodoya E, et al. Transport characteristics of N-acetyl-L-aspartate in rat astrocytes: involvement of sodium-coupled high-affinity carboxylate transporter NaC3/NaDC3-mediated transport system. J Neurochem 2005;93:706–714. [PubMed: 15836629]
12. Truman LA, Bentley KL, Smith EC, et al. ProxTom lymphatic vessel reporter mice reveal Prox1 expression in the adrenal medulla, megakaryocytes, and platelets. Am J Pathol 2012;180:1715–1725. [PubMed: 22310467]
13. Bowyer JF, Thomas M, Patterson TA, et al. A visual description of the dissection of the cerebral surface vasculature and associated meninges and the choroid plexus from rat brain. J Vis Exp 2012;69: e4285.
14. Zhang S, Wang Y, Xu J, et al. HIFα regulates developmental myelination independent of autocrine Wnt signaling. J Neurosci 2021; 41:251–268. [PubMed: 33208471]
15. Moffett JR, Ross B, Arun P, et al. N-Acetylaspartate in the CNS: from neurodiagnostics to neurobiology. Prog Neurobiol 2007;81:89–131. [PubMed: 17275978]
16. Louveau A, Herz J, Alme MN, et al. CNS lymphatic drainage and neuroinflammation are regulated by meningeal lymphatic vasculature. Nat Neurosci 2018;21:1380–1391. [PubMed: 30224810]
17. Johnson NC, Dillard ME, Baluk P, McDonald DM. Lymphatic endothelial cell identity is reversible and its maintenance requires Prox1 activity. Genes Dev 2008;22:3282–3291. [PubMed: 19056883]
18. DeWulf JP, Wiame E, Dorboz I, et al. *SLC13A3* variants cause acute reversible leukoencephalopathy and a-ketoglutarate accumulation. Ann Neurol 2019;85:385–395. [PubMed: 30635937]
19. Gessler DJ, Li D, Xu H, et al. Redirecting N-acetylaspartate metabolism in the central nervous system normalizes myelination and rescues Canavan disease. JCI Insight 2017;2:e90807. [PubMed: 28194442]
20. Feng L, Chao J, Tian E, et al. Cell-based therapy for Canavan disease using human iPSC-derived NPCs and OPCs. Adv Sci 2020;7: 2002155.

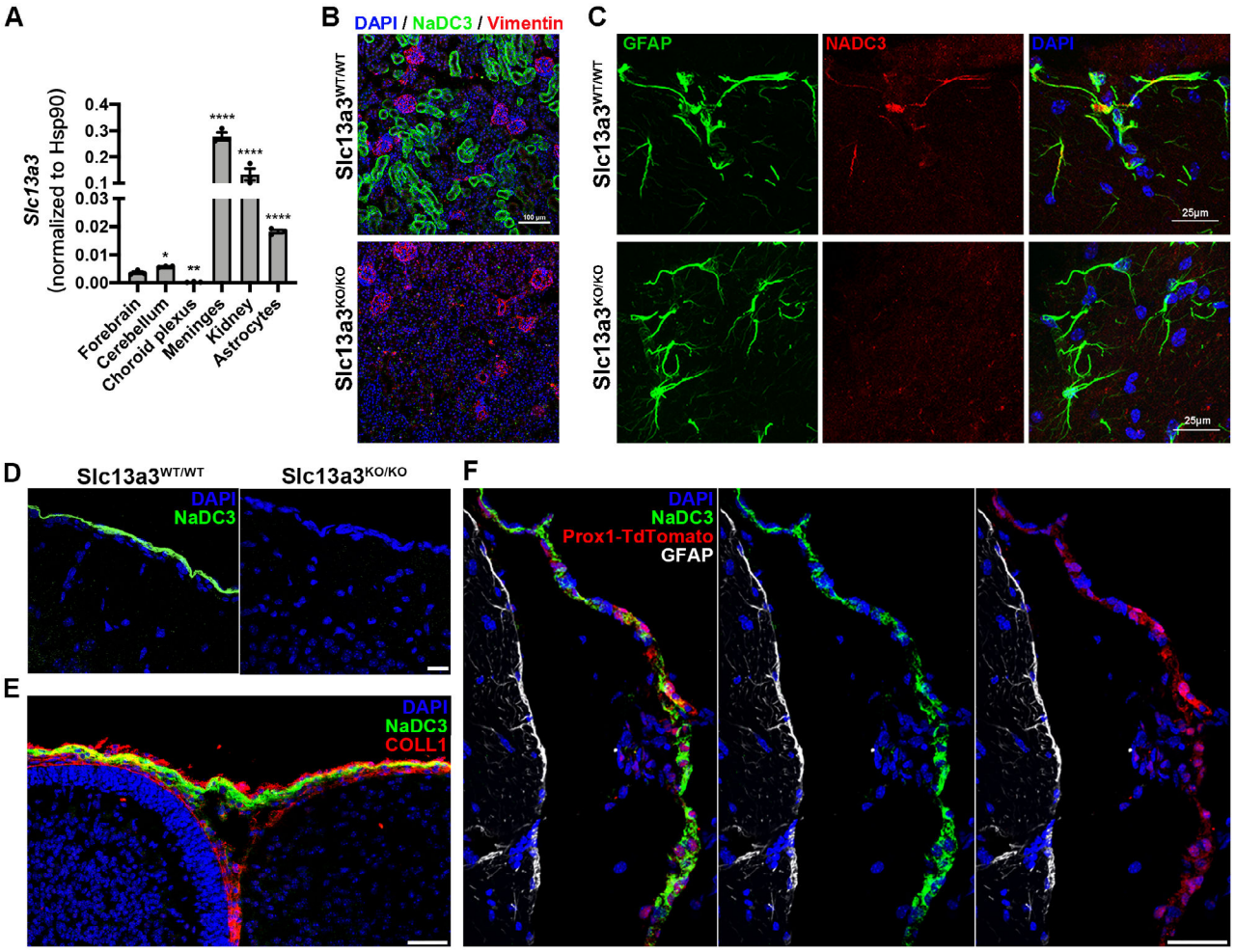

FIGURE 1:

Comparison of the renal and brain *Slc13a3* mRNA and NaDC3 expression between *Slc13a3*$^{WT/WT}$ and *Slc13a3*$^{KO/KO}$ mice. (A) *Slc13a3* mRNA abundance in homogenates prepared from adult forebrain and cerebellar parenchyma, microdissected adult forebrain meninges and choroid plexus, adult mouse kidney, and cultured neonatal mouse astrocyte-enriched cultures. Results are means of determinations from 3 mice or 3 cultures, with vertical lines indicating SEMs. *$p < 0.05$; **$p < 0.01$; ****$p < 0.0001$. (B) Renal tubular NaDC3 immunostaining (green) was detected in *Aspa*$^{WT/WT}$/*Slc13a3*$^{WT/WT}$ mice, but not in *Aspa*$^{WT/WT}$/*Slc13a3*$^{KO/KO}$ mice; glomeruli were vimentin^{+} (red), and nuclei were stained with DAPI (blue); scale bar = 100µm. (C) Some GFAP^{+} astroglia in adult forebrain parenchyma of *Aspa*$^{WT/WT}$/*Slc13a3*$^{WT/WT}$ mice expressed immunoreactive NaDC3, but immunoreactive NaDC3 was not detected in astroglia of *Aspa*$^{WT/WT}$/*Slc13a3*$^{KO/KO}$ mice; scale bars = 25µm. (D) Meningeal immunoreactive NaDC3 was detected in adult *Aspa*$^{WT/WT}$/*Slc13a3*$^{WT/WT}$ mice, but not in *Aspa*$^{WT/WT}$/*Slc13a3*$^{KO/KO}$ mice. (E) Immunoreactive NaDC3 was detected in cerebellar arachnoid mater of neonatal *Aspa*$^{WT/WT}$/*Slc13a3*$^{WT/WT}$ mice, lying below collagen 1α1^{+} immunoreactive cells in dura and above collagen 1α1^{+} immunoreactive cells in pia. (F) NaDC3 (green) and *Prox1* reporter TdTomato (red) immunoreactivities were co-localized in forebrain arachnoid mater of adult

Aspa$^{WT/WT}$/*Slc13a3*$^{WT/WT}$ mice; GFAP^{+} (white) glia limitans is on the left in the panel. Scale bars in D–F = 50μm. Each of the microscopic fields shown in B–F is representative of results from ≥3 individual adult or neonatal mice.

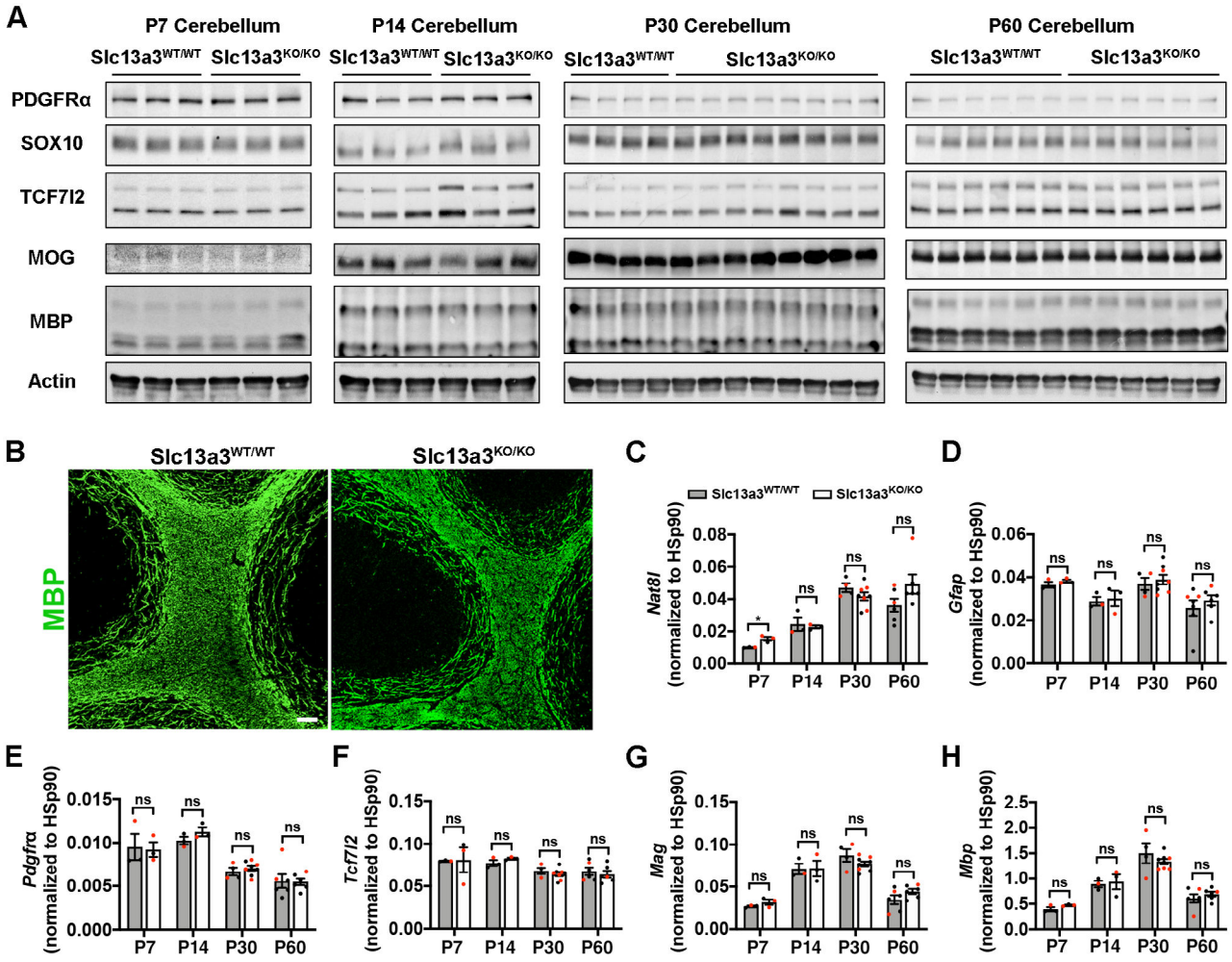

FIGURE 2:

Constitutive *Slc13a3*$^{KO/KO}$ does not alter expression levels of myelin proteins in *Aspa*$^{WT/WT}$ cerebellum between postnatal day (P) 7 and P60, nor alter P7–P60 abundances of neuronal (*Nat8l*), astroglial (*Gfap*), or oligodendroglial lineage (*Pdgfra*, *Tcf7l2*, *Mag*, and *Mbp*) marker mRNAs in *Aspa*$^{WT/WT}$ spinal cord. (A) Western blots of oligodendroglial lineage/myelin protein levels in cerebellar homogenates of *Aspa*$^{WT/WT}$/*Slc13a3*$^{WT/WT}$ and *Aspa*$^{WT/WT}$/*Slc13a3*$^{KO/KO}$ mice on P7, P14, P30, and P60; Western blot lanes from 3 mice of each genotype are shown at each time point. (B) Patterns of MBP immunostaining were similar in cerebella of p60 *Aspa*$^{WT/WT}$/*Slc13a3*$^{WT/WT}$ and *Aspa*$^{WT/WT}$/*Slc13a3*$^{KO/KO}$ mice; scale bar = 50μm. (C–H) Abundances (assayed by qRT/PCR) of *Nat8l*, *Gfap*, *Pdgfra*, *Tcf7l2*, *Mag*, and *Mbp* mRNAs in spinal cord homogenates prepared from *Aspa*$^{WT/WT}$/*Slc13a3*$^{WT/WT}$ and *Aspa*$^{WT/WT}$/*Slc13a3*$^{KO/KO}$ mice on P7, P14, P30, and P60. Each dot (red = female; black = male) in C–H represents an individual mouse. The height of each column indicates the mean, and the vertical lines indicate SEMs. “ns” = nonsignificant differences between the 2 genotypes at each time point.

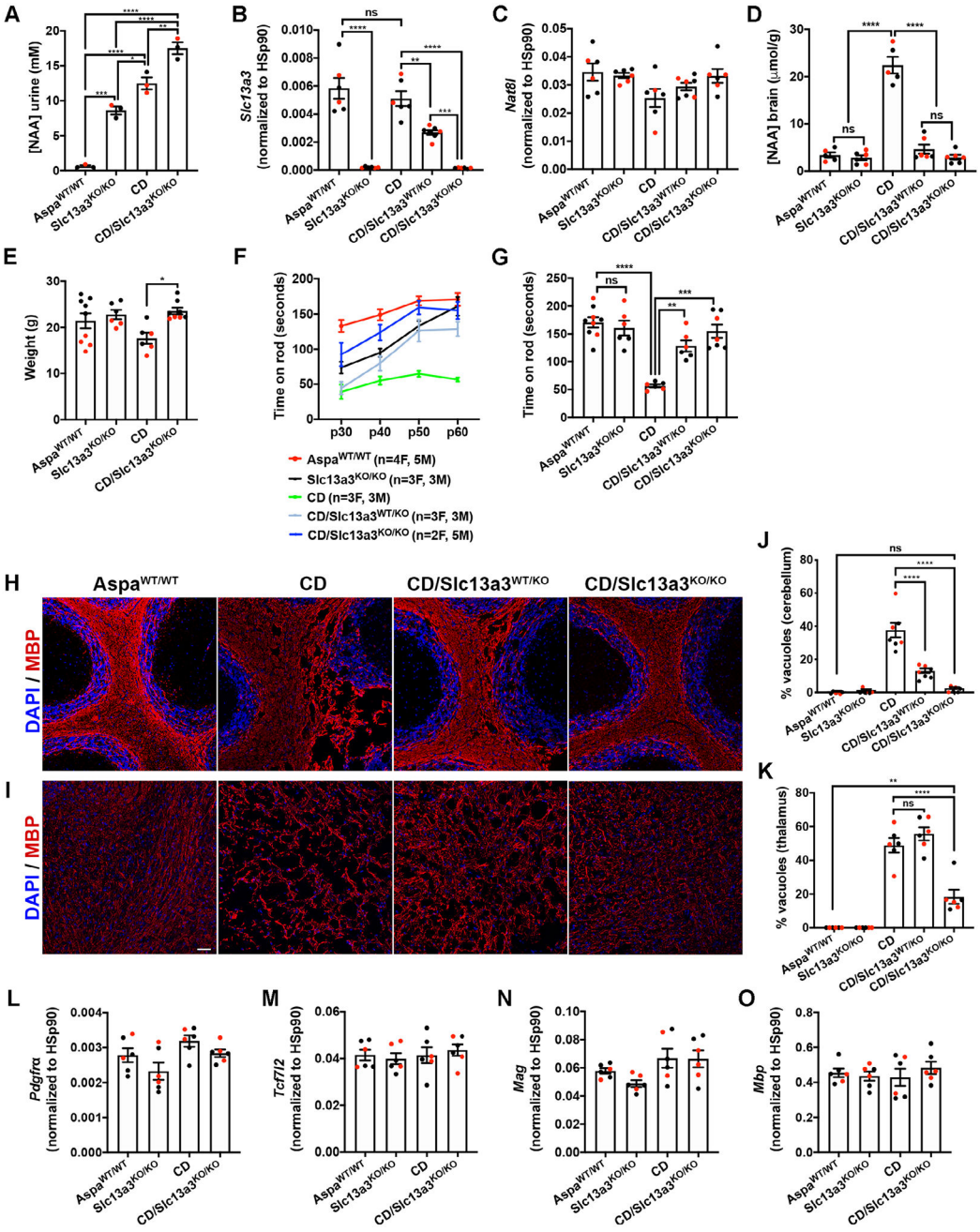

FIGURE 3:

Constitutive *Slc13a3*$^{KO/KO}$ increases urinary *N*-acetyl-L-aspartate (NAA) output, normalizes brain NAA concentration ([NAA_B]), enhances weight gain and rotarod performance, and prevents brain vacuolation in Canavan Disease (CD) mice. (A) Additive effects of CD genotype and *Slc13a3*$^{KO/KO}$ on urinary NAA concentration ($[NAA]_{urine}$). (B) *Slc13a3* mRNA abundances in *Aspa*$^{WT/WT}$/*Slc13a3*$^{WT/WT}$, *Aspa*$^{WT/WT}$/*Slc13a3*$^{KO/KO}$, CD/*Slc13a3*$^{WT/WT}$ (CD), CD/*Slc13a3*$^{WT/KO}$, and CD/*Slc13a3*$^{KO/KO}$ brains. (C) There were no significant effects of *Slc13a3*$^{KO/KO}$ on *Nat8l* mRNA abundance in *Aspa*$^{WT/WT}$ or CD brains. (D) *Slc13a3*$^{KO/KO}$ did not alter [NAA_B] in *Aspa*$^{WT/WT}$ brains, but either *Slc13a3*$^{KO/KO}$ or

Slc13a3$^{WT/KO}$ normalized [NAA_B] in CD brains. (E) Body weights were higher in postnatal day (P) 60 CD/*Slc13a3*$^{KO/KO}$ mice than in P60 CD mice. (F, G) *Slc13a3*$^{KO/KO}$ enhanced accelerating rotarod retention times in CD mice, but not in *Aspa*$^{WT/WT}$ mice; the results at P60 are shown in more detail in G. (H, J) *Slc13a3*$^{KO/KO}$ prevented, and *Slc13a3*$^{WT/KO}$ diminished, cerebellar vacuolation in P60 CD mice. (I, K) *Slc13a3*$^{KO/KO}$ prevented thalamic vacuolation in P60 CD mice, but *Slc13a3*$^{WT/KO}$ did not. Microscopic fields shown in H and I are representative of those in 6 mice in each group. (L–O) *Slc13a3*$^{KO/KO}$ did not significantly alter cerebellar abundances of *Pdgfra*, *Tcf7l2*, *Mag*, or *Mbp* mRNA in P60 CD mice. In A–E, G, and J–O, each dot (red = female; black = male) represents an individual mouse. Analysis of the data in A–D, G, and J–O revealed no significant differences between males and females, but analysis of the data in E indicated that males weighed more than females at P60, and that *Slc13a3*$^{KO/KO}$ increased rotarod retention times in both male and female CD mice ($p < 0.05$ for each sex). Column heights indicate means, and vertical lines indicate SEMs. *$p < 0.05$; **$p < 0.01$; ***$p < 0.001$; ****$p < 0.0001$. Scale bar in I, J = 50 μm. ns = not significant.